Migratory Properties of Naive, Effector, and Memory CD8$^+$ T Cells

Wolfgang Weninger,[1, 2] Maura A. Crowley,[1] N. Manjunath,[1, 3]
and Ulrich H. von Andrian[1, 2]

[1]*The Center for Blood Research, the* [2]*Department of Pathology, and the* [3]*Department of Pediatrics,
Harvard Medical School, Boston, MA 02115*

Abstract

It has been proposed that two different antigen–experienced T cell subsets may be distinguishable by their preferential ability to home to lymphoid organs (central memory cells) or non-lymphoid tissues (effector memory/effector cells). We have shown recently that murine antigen–primed CD8$^+$ T cells cultured in interleukin (IL)-15 (CD8^{IL-15}) resemble central memory cells in phenotype and function. In contrast, primed CD8$^+$ T cells cultured in IL–2 (CD8^{IL-2}) become cytotoxic effector cells. Here, the migratory behavior of these two subsets was investigated. Naive, CD8^{IL-15} cells and, to a lesser degree, CD8^{IL-2} cells localized to T cell areas in the spleen, but only naive and CD8^{IL-15} cells homed to lymph nodes (LNs) and Peyer's patches. Intravital microscopy of peripheral LNs revealed that CD8^{IL-15} cells, but not CD8^{IL-2} cells, rolled and arrested in high endothelial venules (HEVs). Migration of CD8^{IL-15} cells to LNs depended on L-selectin and required chemokines that bind CC chemokine receptor (CCR)7. Both antigen–experienced populations, but not naive T cells, responded to inflammatory chemokines and accumulated at sites of inflammation. However, CD8^{IL-2} cells were 12 times more efficient in migrating to inflamed peritoneum than CD8^{IL-15} cells. Furthermore, CD8^{IL-15} cells proliferated rapidly upon reencounter with antigen at sites of inflammation. Thus, central memory-like CD8^{IL-15} cells home avidly to lymphoid organs and moderately to sites of inflammation, where they mediate rapid recall responses, whereas CD8^{IL-2} effector T cells accumulate in inflamed tissues, but are excluded from most lymphoid organs.

Key words: lymphocyte homing • lymph node • chemokines • adhesion molecules • inflammation

Introduction

Immune responses against pathogens and tumors depend on the ability of lymphocytes to migrate to appropriate places within the body to find their cognate antigen. Naive T cells constantly recirculate between the blood and secondary lymphoid organs such as LNs, Peyer's patches (PPs),* and the spleen (for reviews, see references 1 and 2). When naive T cells are activated by antigen presented on mature dendritic cells (DCs) in these organs, they become lymphoblasts, which proliferate rapidly, and after a few days, acquire effector functions.

The major function of CD8$^+$ effector T cells is thought to be killing of other cells, such as infected or malignant cells expressing viral or tumor antigens (3). Cytotoxicity requires direct contact with the target cell, which can be located anywhere in the body (4). Thus, CTLs must diversify their ability to migrate to different tissues, particularly to sites of inflammation. Irrespective of phenotype, the capacity of a lymphocyte to enter tissues from blood depends upon its ability to adhere to endothelial cells while withstanding hydrodynamic shear stresses exerted by flowing blood. Leukocyte adhesion to endothelial cells is governed by cascades of molecular interactions (1, 2, 5). Tethering and rolling are initiated by members of the selectin family or by $\alpha 4$ integrins. Chemokines displayed on endothelial cells can then activate integrins on rolling leukocytes, bringing cells to firm arrest (sticking [1, 2, 5]). Although rolling, chemoattractant–induced activation,

Address correspondence to Ulrich H. von Andrian, The Center for Blood Research, 200 Longwood Ave., Boston, MA 02115. Phone: 617-278-3130; Fax: 617-278-3190; E-mail: uva@cbr.med.harvard.edu

Abbreviations used in this paper: CCR, CC chemokine receptor; CFSE, carboxyfluorescein diacetate succinimidyl ester; CM, complete media; DC, dendritic cell; GFP, green fluorescent protein; MLN, mesenteric LN; PLN, peripheral LN; HEV, high endothelial venule; PEL, peritoneal exudate leukocyte; PP, Peyer's patch; TRITC, tetramethylrhodamine-5-isothiocyanate.

and sticking may be mediated by several different molecular pathways, in many settings only a single combination will permit efficient recruitment of a leukocyte population to a distinct target tissue. For example, naive T cells express L-selectin (CD62L), the chemokine receptor CCR7, and the β2 integrin LFA-1, which interact respectively with peripheral node addressin (PNAd), the lymphoid chemokine CCL21 (TCA-4, secondary lymphoid tissue chemoattractant [SLC], 6C-kine, exodus 2) and intercellular adhesion molecule (ICAM)-1/-2. This combination of traffic molecules is uniquely found on high endothelial venules (HEVs) of LNs and each specific interaction is essential for efficient homing (6–14).

The factors that govern CTL differentiation and their migratory properties are largely unknown. Until recently, specific markers of effector CTLs, which distinguish them from other CD8+ T cells, have been unavailable (15, 16). We have described a transgenic mouse strain, T-GFP, which permits identification of CD8+ effector cells. In unchallenged T-GFP mice, all naive CD4+ and CD8+ T cells express green fluorescent protein (GFP) at high levels, whereas effector CTLs downregulate GFP expression (15). We have since expanded this model by crossing T-GFP mice to TCR transgenic P14 mice (T-GFPxP14), whose CD8+ T cells recognize the LCMV-derived gp33–41 peptide presented by H2-D^b MHC class I (17). T-GFPxP14 T cells stimulated in vitro with peptide antigen followed by 5 d incubation in a high dose (>5 ng/ml) of IL-2 (henceforth called CD8^{IL-2} cells), express effector cell markers, become GFP−, and display potent antigen specific CTL activity (18). Here, we have made use of this system to examine the migratory behavior of this relatively uniform effector cell population.

A second aim was to compare trafficking of circulating CD8^{IL-2} cells to long-lived memory cells. After antigen has been eliminated nearly all effector cells perish, leaving behind only few antigen-experienced cells, which continue to divide slowly. These memory cells stand guard in blood, epithelial tissues, and lymphoid organs, including LNs, to mediate recall responses if the antigen returns (19–23). How memory cells gain access to LNs is unclear. In sheep models, virtually all T cells in afferent lymphatics have a memory phenotype, whereas most T cells in efferent lymph bear naive T cell markers (24, 25). This proposes the concept that naive T cells home to LNs via HEVs, whereas memory T cells preferentially migrate to nonlymphoid tissues and, subsequently, travel to LNs via afferent lymph vessels. However, in rodents substantial homing of memory T cells to LNs occurs via HEVs (26).

The inherent heterogeneity of antigen-experienced T cells may account for these apparent discrepancies. Indeed, in humans, blood-borne CD45RA− memory cells can be divided into two functionally distinct subsets based on their differential expression of CCR7 (27). Most CCR7+ "central" memory T cells express L-selectin and give rise to effector cells, but lack immediate effector functions when stimulated by antigen. In contrast, CCR7− "effector" memory cells are mostly L-selectin− and display immediate

effector activity. Two functionally distinct populations of CD8+ memory cells have been demonstrated also in mice after infection; one residing in secondary lymphoid tissues and a second in tertiary tissues (23). Both populations were capable of producing IFN-γ, but only the latter showed immediate antigen-specific cytotoxicity ex vivo. While these studies have broadened our understanding of the immune response in general, they beg the question of how memory subsets target different organs. Characterization of the molecular mechanisms of tissue specific trafficking has broad implications for therapy of human disease, including vaccine development.

In mice, the size of the CD8+ memory pool is determined by IL-2 and IL-15: the latter is necessary for memory cell growth and/or survival, whereas the former promotes death of antigen-experienced T cells (28). Furthermore, exposure of peptide-primed T-GFPxP14 T cells to IL-15 in vitro (henceforth called CD8^{IL-15} cells) promotes the generation of central memory-like T cells, which confer long-lived antigen-specific memory upon adoptive transfer into naive hosts (18). Here we made use of CD8^{IL-15} cells to compare their trafficking behavior with naive T cells and effector CD8^{IL-2} cells.

Our studies show that CD8^{IL-15} cells home as well as naive T cells to secondary lymphoid organs, but unlike naive cells, they respond also to inflammatory chemokines and enter peripheral sites of inflammation, where they can rapidly proliferate when they encounter antigen. In contrast, CD8^{IL-2} cells do not migrate to lymphoid tissues other than the spleen, but home more efficiently to sites of inflammation than CD8^{IL-15} cells.

Materials and Methods

Mice. C57BL/6 mice of both sexes were purchased from The Jackson Laboratory or Taconic Farms. P14 transgenic mice, which express a TCR specific for LCMV glycoprotein 33–41 (gp33; reference 17), were obtained from The Jackson Laboratory. L-selectin^{−/−} mice were provided by Dr. Mark Siegelman (University of Texas, Southwestern Medical Center, Dallas, TX; reference 29). T-GFP transgenic mice were generated in our laboratory (15). P14 and L-selectin^{−/−} mice were crossed to T-GFP mice to derive T-GFPxP14 (18) and T-GFPxL^{−/−} mice, respectively. Plt/plt mice on a DDD/1 background and DDD/1-mtv/mtv wild-type control mice were provided by Dr. Akio Matsuzawa, University of Tokyo, Tokyo, Japan. All mice were housed and bred in a specific pathogen free/viral antibody free animal facility. Mice were used between 8 and 16 wk of age, unless stated otherwise. All experiments were in accordance with National Institutes of Health guidelines and approved by the Committees on Animals of both Harvard Medical School and The Center for Blood Research.

Reagents. Human recombinant IL-15 and murine recombinant IL-2 were purchased from R&D Systems. The following rat anti–mouse mAbs were purchased from BD PharMingen: anti-CD3ε; CyChrome (Cy)-labeled anti-CD4 and anti-CD8; FITC-labeled anti-B220; biotinylated anti-Thy1.2; PE-labeled anti-CD44, anti-CD25, anti-α4 integrin, and anti–L-selectin, and allophycocyanin (APC)-conjugated anti-CD8. P-selectin-Ig chi-

mera was obtained from BD PharMingen and the CCL19 (macrophage inflammatory protein [MIP]-3β/ELC)-Ig chimera was a gift from Dr. Timothy Springer (The Center for Blood Research, Boston, MA). The LCMV gp33 peptide (KAVYN-FATC) was synthesized at BioSource International. Murine recombinant SLC (CCL21), monocyte chemoattractant protein (MCP)-1 (CCL2), and regulated upon activation, normal T cell expressed and secreted (RANTES; CCL5) were obtained from R&D Systems.

In Vitro Differentiation of T Cells. Splenocytes from P14 or T-GFPxP14 mice were incubated with gp33 peptide (10 μg/ml) for 1 h at 37°C, washed, and cultured in complete media (CM), which consisted of RPMI 1640 (BioWhittaker) supplemented with 10% FBS (GIBCO BRL), 2 mM L-glutamine (GIBCO BRL), 10 mM pyruvate (GIBCO BRL), penicillin/streptomycin, 10 mM HEPES (GIBCO BRL), and 50 μM β-mercaptoethanol (Sigma-Aldrich). After 48 h, cells were washed and incubated in CM containing either IL-2 (20 ng/ml) or IL-15 (20 ng/ml). Media with fresh cytokines was changed every other day.

Splenocytes from T-GFP mice or T-GFPxL$^{-/-}$ mice were stimulated with anti-CD3ε (1 μg/ml) for 48 h in CM. Thereafter, the same protocol was followed as described for P14 cells. Cytokine-treated cells were used between days 8 and 10 of culture. Before each experiment, the phenotype of the cells was confirmed using cell size and expression of activation markers, L-selectin as well as GFP by flow cytometry (FACScan™; Becton Dickinson).

Phenotyping of Endogenous Memory T Cells. Peripheral blood was obtained from anesthetized aged (18 mo old) T-GFP mice by cardiac puncture. After lysis of red blood cells, single cell suspensions were analyzed by four-color flow cytometry (FACSCalibur™; Becton Dickinson) for their expression of CD8, CD44, CD122, GFP, L-selectin, CD25, and CCL19-Ig binding. Memory CD8$^+$ T cells were defined by high expression of CD44.

Homing Assays. CD8^{IL-15} and CD8^{IL-2} cells were labeled for 20 min with tetramethylrhodamine-5-isothiocyanate (TRITC, 30 μg/ml; Molecular Probes) at 37°C. Thereafter, cells were centrifuged over FBS to remove dead cells and excess TRITC. 5 × 10^7 CD8^{IL-15} or CD8^{IL-2} cells were mixed with 5 × 10^7 freshly isolated splenocytes from T-GFP mice and injected intravenously into recipient mice. An aliquot of the input population was saved for later FACS® analysis to control for variability in the relative frequency of transferred TRITC$^+$ ([TRITC]$_{input}$) and GFP$^+$ ([GFP]$_{input}$) populations. After 1 or 24 h, recipient mice were anesthetized by intraperitoneal injection of 5 mg/ml ketamine HCL (Fort Dodge Animal Health) and 1 mg/ml xylazine (Phoenix Pharmaceutical), and blood was obtained by cardiac puncture. Subsequently, the animals were killed by cervical dislocation. Spleens, peripheral LNs (PLNs), mesenteric LNs (MLNs), and PPs were harvested and passed through wire mesh. Livers and lungs were digested with collagenase type 2 (0.5%; Worthington Biochemical) before passing through wire mesh. Single cell suspensions were analyzed by flow cytometry, and data expressed as percentage of TRITC$^+$ ([TRITC]$_{organ}$) or GFP$^+$ ([GFP]$_{organ}$) cells in the total population of gated live lymphocytes. To correct for differences in the number and composition of injected cells between individual experiments, the homing index (HI) was calculated, where HI = [TRITC]$_{organ}$/[GFP]$_{organ}$:[TRITC]$_{input}$/[GFP]$_{input}$.

Immunofluorescence Staining. Spleens and PLNs were snap-frozen in OCT compound (Triangle Biomedical Science) and stored at −70°C until further use. Acetone-fixed 6-μm cryostat sections were blocked with 0.5% bovine serum albumin (Sigma-Aldrich) in PBS, then incubated with anti-B220 FITC (1 μg/ml) and biotinylated anti-Thy1.2 (1 μg/ml) for 1 h at room temperature. Subsequently, sections were incubated with streptavidin-Cy5 (Jackson ImmunoResearch Laboratories). Slides were analyzed on a confocal laser scanning microscope (Radiance 2000; Bio-Rad Laboratories).

Chemotaxis Assays. 5 × 10^5 CD8^{IL-15} or CD8^{IL-2} T-GFPxP14 cells, or naive T-GFP splenocytes in 100 μl RPMI 1640 plus 10% FBS were loaded in Transwell filters (Costar, Corning, Inc.; 5 μM pores), which were placed in 24-well plates containing 600 μl medium without additives or with chemokines at different concentrations. After incubation for 1 h at 37°C, cells in the bottom well were collected and counted by flow cytometry. Chemotactic indices were calculated as the number of migrated cells in wells containing chemokines divided by the number of migrated cells in wells containing medium alone.

Peritonitis. Peritonitis was induced in C57BL/6 mice by intraperitoneal injection of 0.5 ml (1:1, vol/vol) emulsified IFA (Sigma-Aldrich) in PBS. After 72 h, mice received intravenous injection of either a mixture of 2.5 × 10^7 TRITC-labeled CD8^{IL-2} cells plus 2.5 × 10^7 carboxyfluorescein diacetate succinimidyl ester (CFSE; Molecular Probes)-labeled CD8^{IL-15} cells, or a mixture of 2.5 × 10^7 TRITC-labeled CD8^{IL-15} cells plus 4 × 10^7 naive T-GFP splenocytes containing ∼1.5 × 10^7 GFP$^+$ naive cells. After 24 h, mice were killed and peritoneal exudate leukocytes (PELs) harvested by PBS lavage. At the same time, blood and PLNs were also harvested and the distribution of each subset was assessed as described above. To determine responses to gp33 peptide, mice received 2.5 × 10^7 CFSE-labeled CD8^{IL-15} cells from P14 mice. 24 h later, peritonitis was induced by injection of IFA in the absence or presence of gp33 peptide (50 μg). PELs were harvested 72 h later and analyzed by flow cytometry.

Intravital Microscopy. Intravital microscopy of the subiliac (superficial inguinal) LN microcirculation was performed as described (8, 30). Briefly, young adult C57BL/6 mice (8–10 wk) were anesthetized and the right femoral artery catheterized with PE-10 polyethylene tubing. After dissection of the left subiliac LN, animals were transferred to an intravital microscope (IV-500; Micron Instruments) equipped with infinity corrected water-immersion objectives (ZEISS). Small boluses of TRITC-labeled CD8^{IL-2} cells or calcein-labeled CD8^{IL-15} cells were retrogradely injected into the femoral artery catheter. Cells that entered the LN microvasculature were visualized through appropriate filters using fluorescent epi-illumination from a video-triggered xenon arc stroboscope (Chadwick-Helmuth). Video images were recorded using a low-lag silicon-intensified target camera (VE1000SIT; Dage, MTI), a time base generator (For-A Corp. Ltd.) and a Hi8 VCR (Sony).

Image Analysis. Cell behavior was determined by off-line analysis of video tapes (31). The rolling fraction for each individual venule was measured as the percentage of T cells that interacted detectably with the vascular wall in the total number of fluorescent (rolling plus noninteracting) cells that passed a vessel during the observation period. The sticking fraction was defined as the percentage of total cells that became firmly adherent for ≥30 s while passing a venule within the observation period.

Statistical Analysis. All data are presented as mean ± SEM, unless otherwise indicated. Homing indices of IL-2 versus IL-15–treated cells to individual organs was compared using the unpaired Student's *t* test. Rolling and sticking fractions of IL-2 versus IL-15–treated cells in the same PLNs were compared using the paired Student's *t* test. Significance was reached at $P < 0.05$.

Results

Exposure of Antigen-primed CD8$^+$ T Cells to IL-2 or IL-15 Generates Effector or Central Memory-like Cells, Respectively. We have recently described an in vitro system to generate antigen-experienced T cells that possess phenotypic and functional features of in vivo generated effector CTL and central memory CD8$^+$ T cells (18). T-GFP mice were crossed with P14 TCR transgenic mice (T-GFPxP14). When splenocytes from these mice are primed with antigen and cultured in IL-2 (20 ng/ml $\cong$ 1,000 U/ml; CD8^{IL-2}) for 1 wk they acquire an effector phenotype; they have a blastoid morphology, are GFP$^-$L-selectin$^{lo/-}$CD44^{hi}CD25^{hi}CCR7$^-$, and display potent antigen-specific cytotoxicity. In contrast, when primed cells are cultured instead in 20 ng/ml IL-15 (CD8^{IL-15}), they phenotypically resemble a subset of memory cells that has been described in human peripheral blood (27); they are of intermediate size, are CD44^{hi}L-selectin$^+$CD25^{int}CCR7$^+$, and most cells ($\sim$70%) remain GFP$^+$ (Table I). Most importantly, CD8^{IL-15} cells possess little immediate CTL activity in vitro, but when transferred into naive syngeneic hosts, they survive for long periods of time and mount a rapid antigen-specific recall response to viral and bacterial infections. Thus, CD8^{IL-15} cells phenotypically and functionally meet the criteria attributed to memory cells, while CD8^{IL-2} cells represent fully differentiated effector CTL (18).

The findings in the T-GFPxP14 TCR transgenic system (18) were confirmed in the present study (Table I). In addition, to test the effects of our protocol in a normal T cell repertoire, splenocytes from T-GFP mice were stimulated with anti-CD3ϵ (1 μg/ml) for 48 h followed by IL-2 or IL-15 treatment as described above. The resulting polyclonal populations of effector and memory T cells consisted mostly of CD8$^+$ cells (82 and 93% after culture in IL-2 and IL-15, respectively) whose phenotype and migratory behavior were indistinguishable from peptide-primed P14 TCR transgenic cells (data not shown). Thus, data from experiments using differentiated T-GFP or P14xT-GFP cells were pooled in some of the experiments described below.

CD8^{IL-15} Cells Resemble a Subset of Circulating Memory Cells In Vivo. We next compared the phenotype of CD8^{IL-15} cells to endogenous CD8$^+$ memory cells isolated from blood of aged ($\sim$18 mo old) T-GFP mice ($n = 3$). Memory CD8$^+$ T cells in mice are defined by their high expression of CD44 and CD122 (28). A distinct population of CD8$^+$CD44^{hi}CD122^{hi} cells was readily detectable in the blood of T-GFP mice (data not shown). As the CD44^{hi} cells were those that also expressed high levels of CD122, and vice versa, we used high expression of CD44 to define memory cells for four-color phenotyping. Among these circulating CD8$^+$ memory cells 72.5 $\pm$ 6.9% were GFP$^+$. Nearly all of the GFP$^+$ memory cells expressed L-selectin and bound CCL19-Ig, whereas less than half of the GFP$^-$ memory cells expressed L-selectin or bound CCL19-Ig (Table II). The activation marker CD25 was expressed on a minority of CD8$^+$ memory cells (not shown). These data suggest that, similar to what has been described in humans, there exist (at least) two populations of circulating memory cells in mice; the largest subset displays a central memory phenotype, i.e., cells in this subset are CD44^{hi}L-selectin$^+$CCR7$^+$ and, in T-GFP mice, also express GFP. In vitro generated CD8^{IL-15} cells strikingly resemble these cells (Tables I and II). As current technology does not allow us to isolate sufficiently large and homogeneous effector and central memory cell populations directly from blood or other organs of immunized mice to analyze their migratory properties, we generated CD8^{IL-2} and CD8^{IL-15} cells for such studies.

CD8^{IL-15} Cells, but Not CD8^{IL-2} Cells Home to LNs and PPs. To analyze the migratory behavior of in vitro generated effector and central memory cells, CD8^{IL-2} and CD8^{IL-15} cells were labeled with the red fluorescent dye TRITC, which does not interfere with in vivo migration of labeled cells (reference 32, and our unpublished results). As a reference population, we used freshly isolated splenocytes from young adult T-GFP mice, which contain $\sim$35% GFP$^+$ naive T cells, with a CD4$^+$:CD8$^+$ ratio of $\sim$2:1. This ratio

Table I. *Expression of GFP, Activation Markers, Adhesion Molecules, and CCR7 on CD8^{IL-2} and CD8^{IL-15} Cells*

	GRP %	CD44^{hi} % (MFI)	CD25 % (MFI)	L-selectin % (MFI)	P-selectin-Ig %	CCL19-Ig % (MFI)
Naive	99 $\pm$ 1	N/A	0.5 $\pm$ 0.7 (51 $\pm$ 5)	99 $\pm$ 1 (1,100 $\pm$ 16)	0.5 $\pm$ 0.3	96 $\pm$ 2 (264 $\pm$ 11)
CD8^{IL-2}	6 $\pm$ 1	97 $\pm$ 1 (1,479 $\pm$ 651)	98 $\pm$ 1 (2,081 $\pm$ 1,054)	25 $\pm$ 12 (398 $\pm$ 234)	71 $\pm$ 18	20 $\pm$ 11 (73 $\pm$ 19)
CD8^{IL-15}	71 $\pm$ 5	82 $\pm$ 12 (661 $\pm$ 221)	94 $\pm$ 3 (178 $\pm$ 123)	93 $\pm$ 8 (1,953 $\pm$ 629)	4 $\pm$ 5	87 $\pm$ 8 (251 $\pm$ 28)

CD8^{IL-2} and CD8^{IL-15} cells were generated from P14xT-GFP or P14 mice as described in Materials and Methods. Naive splenocytes (defined as CD44$^{lo/-}$ were freshly prepared from P14xT-GFP mice. The phenotype of the cells was assessed using FACS® (FACScan™). Shown are the percentages (mean $\pm$ SEM) and mean fluorescence intensity (MFI) $\pm$ SEM of marker positive cells in the total population of three to seven experiments.

Table II. *Phenotype of Endogenous CD8+ Peripheral Blood Memory T Cells*

	CD44 MFI	L-selectin % (MFI)	CCL-19-Ig % (MFI)
GFP+CD44−/lo	35 ± 10	90 ± 5 (527 ± 111)	96 ± 2 (154 ± 72)
GFP+CD44hi	891 ± 39	92 ± 2 (854 ± 168)	93 ± 4 (138 ± 45)
GFP−CD44hi	1,087 ± 69	42 ± 12 (486 ± 36)	43 ± 13 (118 ± 17)

Leukocytes were isolated from peripheral blood of aged T-GFP mice (>1.5 yr, $n = 3$). The cells were stained as described in Materials and Methods and phenotyped using 4-color FACS® (FACSCalibur™). Gates were set on either CD8+CD44−/lo (naive) or CD8+CD44hi (memory) cells. The latter constituted 27.6 ± 1.9% of the total pool of circulating CD8+ T cells. GFP+ cells represented 72.5 ± 6.9% of total CD8+ memory cells. Shown are the percentages (mean ± SEM) and/or mean fluorescence intensity (MFI) ± SEM of marker positive cells. Note that different flow cytometers were used in Tables I and II. Thus, the absolute magnitude of MFI values in the two tables cannot be compared directly.

was not significantly altered in the population of GFP+ cells that were recovered from recipient tissues after adoptive transfer ($n = 10$ animals, $P > 0.05$ for all organs tested). Therefore, GFP+ T-GFP cells were considered a uniform population of naive T cells that served as an inter-nal standard to which the trafficking of cytokine treated cells was compared.

5×10^7 TRITC-labeled CD8IL-15 or CD8IL-2 cells were mixed with naive T-GFP cells (5×10^7 splenocytes) and injected intravenously into naive C57BL/6 mice. Recipient organs were harvested 24 h later and single cell suspensions were analyzed by flow cytometry (Fig. 1). As shown in Fig. 1 A, all of the injected T cell populations were present in the host circulation. However, the average frequency of the two stimulated subsets in blood was only ~40% of that of naive T-GFP cells. This skewed subset ratio in blood, despite the fact that smaller numbers of GFP+ cells were injected, was apparent immediately after intravenous injection and throughout the 24-h homing period (data not shown) indicating that many cytokine treated cells were selectively retained in host tissues. Indeed, the ratio of cytokine-treated to naive T cells was much higher in the recipients' liver and lungs (Fig. 1 B). Despite the tendency for larger numbers of CD8IL-2 cells than CD8IL-15 cells to accumulate in these two organs, this difference was not statistically significant. The lower blood levels of the larger, stimulated cells may have been due to mechanical sequestration in pulmonary and portal microvessels, which have low perfusion pressure. However, a contribution by specific molecular interactions cannot be excluded.

No significant difference was found in the concentration of CD8IL-2 and CD8IL-15 cells in peripheral blood of recipient mice (Fig. 1 C). In contrast, CD8IL-15 cells were more frequent than CD8IL-2 cells in the spleen where the two populations constituted 8.1 ± 1.8% and 2.5 ± 1.1% of res-
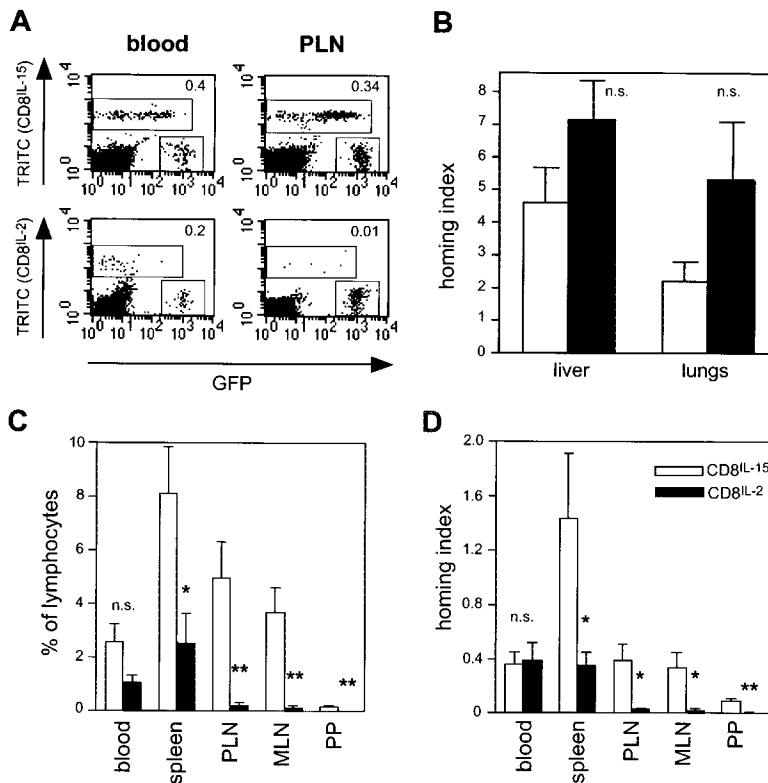

Figure 1. Primed CD8+ T cells differentiated with IL-15, but not with IL-2, home to LNs. Splenocytes from T-GFPxP14 mice ($n = 4$) or from T-GFP mice ($n = 2$) were stimulated with gp33 peptide or anti-CD3ε, respectively, and cultured for 6–8 d in the presence of IL-2 (black bars) or IL-15 (white bars). 5×10^7 TRITC-labeled cells from either cytokine-treated population were mixed with 5×10^7 fresh T-GFP splenocytes (as an internal standard) and injected intravenously into naive C57BL/6 recipients. The ratio of homed TRITC+ cells to GFP+ TRITC− cells in different tissues was analyzed by flow cytometry 24 h later (gates were set on live lymphocytes). As cytokine-treated primed T-GFPxP14 and T-GFP cells behaved identically, the results were pooled. (A) Representative two-color dot plots of adoptively transferred T cell subset frequencies in peripheral blood leukocytes (left) and PLNs (right) of two recipient mice. Adoptively transferred CD8IL-15 cells (top panels) or CD8IL-2 cells (bottom panels) are both readily detectable in blood, but only CD8IL-15 cells are found in significant numbers in PLNs. The homing index (i.e., the ratio of TRITC+:GFP+ events in respective gates divided by the ratio of TRITC+:GFP+ cells in the mixture before adoptive transfer) is shown in the upper right corner of each panel. (B) Homing indices of CD8IL-15 cells and CD8IL-2 cells versus naive T-GFP cells in the lungs and liver. (C) Frequency of homed cells in blood and secondary lymphoid organs. Bars represent the percentage of homed TRITC+ cells in gated lymphocyte populations. (D) Homing indices of CD8IL-15 cells and CD8IL-2 cells versus naive T-GFP cells in lymphoid organs. *$P < 0.05$; **$P < 0.01$; n.s., not significant. Bars represent mean ± SEM of results from six mice.

ident lymphocytes, respectively ($P = 0.022$; $n = 6$ animals). This difference in tissue-specific homing was even more dramatic in other secondary lymphoid organs. The frequency of CD8[IL-15] cells in PLNs was 23.1-fold higher than that of CD8[IL-2] cells ($5.0 \pm 1.33\%$ vs. $0.22 \pm 0.09\%$; $P = 0.005$), and a 25.8-fold difference was found in MLNs ($3.66 \pm 0.93\%$ vs. $0.14 \pm 0.06\%$; $P = 0.003$). Although smaller numbers of both populations homed to PPs, there were significantly more CD8[IL-15] cells than CD8[IL-2] cells in those organs as well ($0.16 \pm 0.04\%$ vs. $0.02 \pm 0.007\%$, $P = 0.009$). It was theoretically possible that some effector cells homed rapidly to LNs either directly or via peripheral tissues and afferent lymphatics, but escaped detection at 24 h after transfer due to either subsequent exit from the LNs or a limited lifespan. However, in short term (1 h) homing experiments, the percentage of recovered CD8[IL-2] cells in PLNs was $0.03 \pm 0.01\%$ of total lymphocytes, indicating that there are no alternative routes by which circulating effector cells could rapidly migrate into normal PLNs.

To compare the homing potential of stimulated cells relative to naive T cells and also to account for potential differences in cell input, we calculated the homing index, which was defined as the ratio of TRITC^{+}:GFP^{+} cells in a tissue divided by the ratio of TRITC^{+}:GFP^{+} cells in the input population (Fig. 1 D). Homing indices of CD8[IL-15] cells versus naive T-GFP cells were comparable in blood, PLNs, and MLNs. If one takes into account the difference in circulating T cell counts, this suggests that CD8[IL-15] cells homed equally well to LNs as naive T cells. In contrast, the ratio of CD8[IL-2] to T-GFP cells was very low in all of these lymphoid organs. Interestingly, the homing index of CD8[IL-15] versus naive cells in the spleen was 1.43 ± 0.48, whereas that of CD8[IL-2] versus naive cells was 0.35 ± 0.1, which is comparable to ratio of CD8[IL-2] versus naive cells in blood (0.38 ± 0.14). Thus, compared with naive T cells, CD8[IL-2] cell recruitment to the spleen is similar, while

CD8[IL-15] cell migration to the spleen is enhanced. The homing indices for both cytokine-treated subsets in PPs were much lower than in the blood and other organs examined (CD8[IL-15]: 0.1 ± 0.01; CD8[IL-2]: 0.01 ± 0.004) indicating that PPs are preferentially a target for naive T cells. Taken together, these data demonstrate that CD8[IL-15] cells migrate avidly to lymphoid organs, whereas CD8[IL-2] cells are excluded from all lymphoid tissues except the spleen.

CD8[IL-15] and CD8[IL-2] Cells Localize to T Cell Areas in the Spleen and LNs. While no single trafficking molecule appears to be essential for T cell homing from blood to the spleen, cell entry into T cell zones requires active migration within splenic compartments, which involves the concerted action of adhesion molecules and chemokine receptors (33, 34). Having established that substantial numbers of antigen-experienced T cells accumulate in the spleen, we sought to determine whether this process was a specific migratory event or represented passive trapping of the cells in splenic red pulp. Spleens and PLNs from three mice were harvested 24 h after adoptive transfer of TRITC-labeled CD8[IL-15] or CD8[IL-2] cells and cryostat sections were stained for B220 and Thy-1 to visualize host B and T cells, respectively. As depicted in Fig. 2, the vast majority (>90%) of homed CD8[IL-15] cells localized specifically to T cell areas in both lymphoid organs. CD8[IL-2] cells were also preferentially found in splenic T cell areas ($61 \pm 2\%$ of TRITC^{+} cells). However, this population appeared more scattered and sizable fractions localized to the red pulp ($21 \pm 2\%$) and the B cell area ($18 \pm 1\%$). Very few CD8[IL-2] cells were found in PLNs, mostly localized to the T cell area.

Homing of CD8[IL-15] Cells to LNs Requires L-Selectin and CCR7 Agonists. While there is an abundance of data on the pivotal role of L-selectin and CCR7 for naive T cell homing to PLNs (6–8, 14, 35), the mechanisms by which memory cells gain access to these organs are poorly understood. As CD8[IL-15] cells expressed high levels of L-selectin
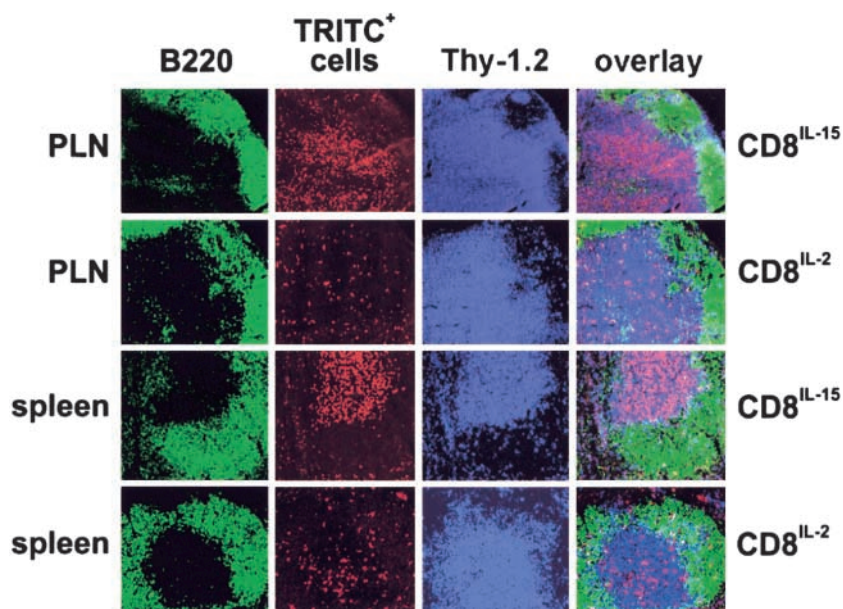

Figure 2. Localization of homed CD8[IL-15] and CD8[IL-2] cells in PLNs and spleen. Cryostat sections of PLNs (top two rows) and spleen (bottom two rows) 24 h after adoptive transfer of TRITC-labeled CD8[IL-15] cells or CD8[IL-2] cells were stained with anti–B220-FITC (green) and Thy-1.2-biotin followed by Cy5-conjugated streptavidin (blue) to localize B cell follicles and T cell areas, respectively. TRITC-labeled homed donor cells are identified by red fluorescence. Micrographs are representative of organs from three different recipient mice.
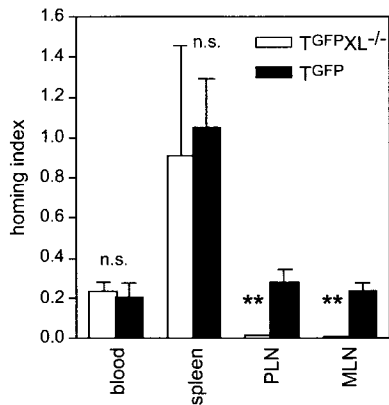
Figure 3. L-selectin is essential for CD8[IL-15] cells to home to LNs. Splenocytes from T-GFPxL^{-/-} mice (white bars) or T-GFP mice (black bars) were stimulated with anti-CD3ε for 2 d and then cultured in the presence of IL-15 (20 ng/ml). After 7 d, 5×10^7 TRITC-labeled CD8[IL-15] cells from each strain were mixed with 5×10^7 freshly isolated T-GFP splenocytes and injected intravenously into C57BL/6 recipients. The frequency of TRITC^{+} cells in blood and secondary lymphoid organs was analyzed 24 h later. The homing index was determined as described in Fig. 1. Bars reflect mean ± SEM from three independent experiments. Homing was compared using the unpaired Student's t test. **$P < 0.01$; n.s., not significant.

and avidly bound the CCR7 ligand CCL19 (Table I), it seemed plausible that the pronounced LN tropism of this subset also relied on L-selectin and CCR7. To test this hypothesis, we crossed T-GFP mice to L-selectin^{-/-} mice (T-GFPxL^{-/-}) and stimulated splenocytes from these animals or from T-GFP mice (as a control) with anti-CD3ε followed by culture in IL-15 for 8 d. TRITC-labeled CD8[IL-15] cells were then mixed with T-GFP splenocytes and used for homing assays in C57BL/6 recipients. T-GFPxL^{-/-} CD8[IL-15] cells failed to home to PLNs (homing index: 0.013 ± 0.003) and MLNs (homing index: 0.01 ± 0; Fig. 3). In contrast, the homing indices of T-GFP CD8[IL-15] and T-GFPxL^{-/-} CD8[IL-15] cells in peripheral blood and spleen were comparable.

The chemokine CCL21 is highly expressed in HEVs and has been shown to trigger rapid integrin-mediated arrest of naive T cells that roll in these vessels (13, 14, 35). CCL21 as well as the related lymphoid chemokine CCL19 signal T cells via CCR7 (36). The LN-expressed genes for both of these chemokines are absent in plt/plt mice, which have a severe defect in naive T cell homing to nonsplenic secondary lymphoid organs (10, 14, 37–40). To determine whether these CCR7 agonists are also required for migration of CD8[IL-15] cells to LNs, homing assays with CD8[IL-15] cells from T-GFPxP14 mice were performed using either plt/plt mice or wild-type DDD1-mtv/mtv mice as recipients. As PLNs in plt/plt mice contain ~80% fewer resident lymphocytes than wild-type mice (40), a given number of homed cells would be more diluted in wild-type than in plt/plt PLNs (14). Therefore, the absolute numbers of homed cells per 10^6 injected cells in each organ was assessed (Fig. 4). As shown previously, significantly larger numbers of naive T-GFP cells homed to plt/plt spleens compared with DDD1-mtv/mtv mice ($P < 0.05$). CD8[IL-15] cells also tended to home more to plt/plt spleens, but this difference did not reach statistical significance ($P = 0.25$). Compared with wild-type mice, PLNs in plt/plt mice contained 95 and 80% fewer homed naive T-GFP cells and CD8[IL-15] cells, respectively ($P < 0.01$ for both). Similarly, an 88 and 89% reduction in homing to MLNs was seen for naive T-GFP cells and CD8[IL-15] cells, respectively ($P < 0.01$). The inability of T-GFP cells and CD8[IL-15] cells to home from the blood to LNs in plt/plt mice was mirrored by a marked elevation in the frequency of these cells among circulating leukocytes (naive T-GFP in blood of wild-type versus plt/plt mice: 1.1 ± 0.2 vs. 3.2 ± 0.2%; $P < 0.0001$; CD8[IL-15]: 1.4 ± 0.1 vs. 5.8 ± 0.6%, $P < 0.0001$).

CD8[IL-15] Cells Roll and Stick in HEVs of PLNs. The results above show that CD8[IL-15] cells rely on similar adhesion pathways as naive T cells, namely L-selectin and CCR7, to home to LNs. As naive T cells enter PLNs exclusively via HEVs, it seemed likely that HEVs are also the port of entry for CD8[IL-15] cells. To test this hypothesis, we employed an intravital microscopy model that allows us to analyze lymphocyte behavior in HEVs of subiliac LNs in anesthetized mice (31). Based on our previous observations, which have shown that naive T cells interact mainly with small paracortical venules (branching orders III to V)
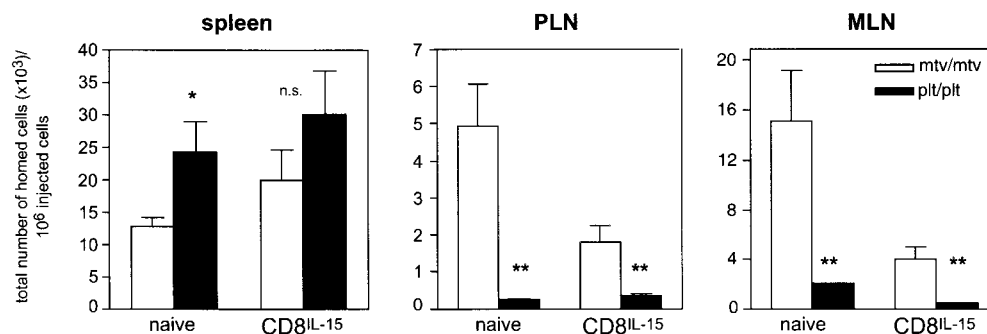

Figure 4. Homing of CD8[IL-15] cells to LNs is impaired in plt/plt mice. Splenocytes from T-GFPxP14 mice were stimulated with gp33 peptide and cultured in IL-15 for 6–8 d. TRITC-labeled CD8[IL-15] cells (5×10^7) were mixed with 5×10^7 freshly isolated T-GFP splenocytes and adoptively transferred into either wild-type DDD1-mtv/mtv (white bars) or plt/plt recipients (black bars). The absolute number of homed cells in spleens, PLNs, and MLNs was calculated by multiplying the frequency of fluorescent cells (assessed by flow cytometry) with the total number of resident lymphocytes in each organ. Data are shown as number of homed cells per 10^6 cells injected. Bars reflect mean ± SEM ($n = 5$ recipients of each strain). Homing was compared using the unpaired Student's t test. *$P < 0.05$; **$P < 0.01$, n.s., not significant.
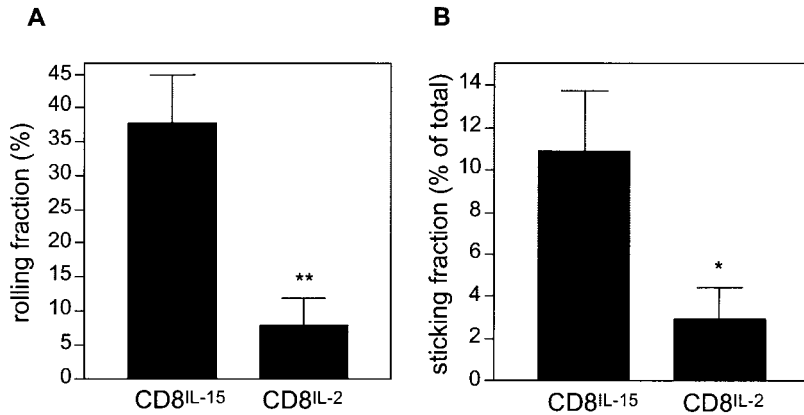
959   Weninger et al.

A

B

Figure 5. Differential rolling and sticking of CD8^IL-15 and CD8^IL-2 cells in PLN HEVs. CD8^IL-15 cells and CD8^IL-2 cells were labeled with calcein and TRITC, respectively, and successively injected into the right femoral artery of an anesthetized mouse. Interactions of injected cells with HEV in surgically prepared left subiliac LNs were studied by epi-fluorescence intravital microscopy as described (reference 31). (A) Rolling fractions (the percentage of rolling cells in the total flux of cells passing a venule) and (B) sticking fractions (the percentage of cells that arrested for ≥30 s in the total flux) of both T cell populations were analyzed in the same 11 HEVs of 4 animals. Bars represent means ± SEM. Data were compared using the paired Student's t test. $*P < 0.005$; $**P < 0.001$.

of the venular tree rather than with collecting venules (order I and II) in the medulla (8), we focused our analysis on paracortical venules. TRITC–labeled CD8^IL-2 and calcein-labeled CD8^IL-15 cells were injected retrogradely into the right femoral artery of C57BL/6 mice and the cells were consecutively recorded while passing through the left subiliac LN. A total of 11 HEVs (8 order III and 3 order IV venules) in 4 animals were analyzed. The mean rolling fraction for CD8^IL-15 cells in these vessels was 37.8 ± 7.1%, whereas only 7.8 ± 4.0% of CD8^IL-2 cells rolled in the same HEVs ($P < 0.001$; Fig. 5 A). The mean sticking fraction for CD8^IL-15 and CD8^IL-2 cells was 10.9 ± 2.8% and 2.9 ± 1.5%, respectively ($P < 0.005$; Fig. 5 B). This demonstrates that CD8^IL-15 cells, but not CD8^IL-2 cells interact avidly with PLN HEVs and provides a likely mechanism for the differential migratory behavior of these two subsets in homing assays.

Both CD8^IL-15 and CD8^IL-2 Cells Respond to Inflammatory Chemokines and Are Recruited to Sites of Inflammation. Having shown that CD8^IL-15 cells, but not CD8^IL-2 cells bind the CCR7 agonist CCL19 by flow cytometry and home to PLNs of wild-type, but not plt/plt mice, chemotaxis assays were performed to compare directly the cells' ability to respond to the second CCR7 agonist, CCL21, which is critical for naive T cell homing to PLNs (14). As expected,

CD8^IL-15 cells showed a prominent migratory response to CCL21, whereas CD8^IL-2 cells responded poorly (Fig. 6). Thus, CD8^IL-15 cells express functional CCR7 (although their chemotactic index was lower than that of naive T cells; data not shown), and the CCR7− CD8^IL-2 cells do not possess alternative means to respond to CCL21.

Different subsets of antigen experienced T cells are known to express distinct repertoires of receptors for chemokines expressed at sites of inflammation (for reviews, see references 2, 36, and 41). We therefore tested the response of cytokine-treated cells to the inflammatory chemokines CCL5 (RANTES) and CCL2 (MCP-1, JE). Both CD8^IL-15 and CD8^IL-2 cells responded similarly to CCL5, whereas CCL2 was more potent, but equally efficient in attracting CD8^IL-2 cells compared with CD8^IL-15 cells. This suggested that both subsets might be able to travel to inflamed tissues.

To assess the ability of CD8^IL-15 cells and CD8^IL-2 cells to migrate to sites of inflammation, we induced acute peritonitis in mice by injecting IFA, a model shown previously to induce the migration of polarized CD4+ effector T cells to the peritoneal cavity (42). IFA was injected intraperitoneally into C57BL/6 mice and fluorescently labeled T cells were injected intravenously 72 h later. As the degree of inflammation was somewhat variable between animals, we compared the migratory potential of two differentially la-
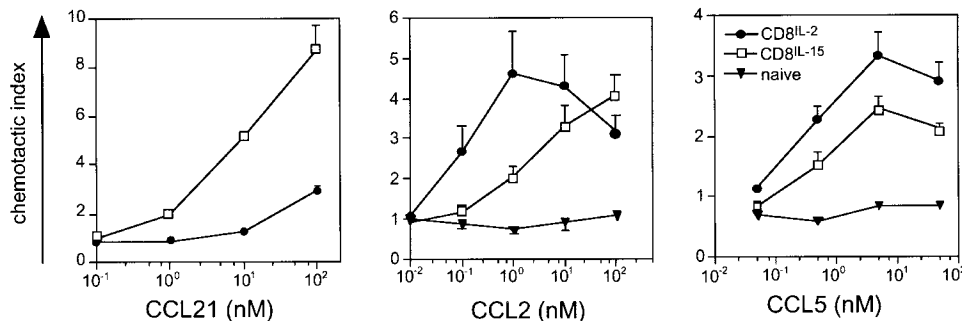

Figure 6. Both CD8^IL-15 and CD8^IL-2 cells respond to inflammatory chemokines. CD8^IL-2 (●), CD8^IL-15 (□), or naive splenocytes (▼) were loaded into Transwell filter inserts (5 × 10^5 cells/well), which were placed in 24-well plates containing 600 μl of medium with different concentrations of CCL21, CCL5 (RANTES), or CCL2 (MCP-1). Chemotactic indices were calculated as the ratio of the number of cells that migrated toward a chemokine divided by the number of spontaneously migrating cells recovered from wells that contained medium without chemokine. Data reflect mean ± SEM of at least two duplicate experiments.

beled cell populations that were coinjected into the same animal. One group of mice received TRITC-labeled CD8[IL-15] cells together with naive T-GFP splenocytes and a second group CFSE-labeled CD8[IL-15] cells and TRITC-labeled CD8[IL-2] cells. 24 h after transfer, peripheral blood leukocytes, PLNs, and PEL were harvested, and analyzed by flow cytometry (Fig. 7, A and B). In agreement with previous reports (42), naive T cell migration was poor; on average, only 349 ± 84 naive T-GFP cells per mouse migrated into the peritoneal cavity (Fig. 7 C). In contrast, substantial numbers of CD8[IL-15] cells were found ($9,708 \pm 2,591$/mouse; $P < 0.01$ versus naive cells). Significantly larger numbers of CD8[IL-2] cells were recovered from PEL, when coinjected with CD8[IL-15] cells ($40,181 \pm 10,574$ CD8[IL-2] cells/mouse vs. $14,851 \pm 4,541$ CD8[IL-15] cells/mouse; $P < 0.05$). As determined, the three T cell populations are retained to different degrees in the liver and lungs (Fig. 1 B) and their concentration in peripheral blood is quite variable (Fig. 1 C). To correct for potential skewing of our results due to dissimilar delivery of blood-borne cells

to the peritoneum, we divided the ratio of each pair of cell populations in PEL by their ratio in blood. After thus normalizing for differences in blood cell counts, CD8[IL-15] cells were found to home 15.3 ± 4.8-fold more frequently to inflamed peritoneum than naive T cells, whereas homing of CD8[IL-2] cells was 11.7 ± 2.8-fold greater than that of CD8[IL-15] cells.

These data suggested that not only CD8[IL-2] effector cells, but also CD8[IL-15] central memory-like cells can migrate to inflamed tissues. However, CD8[IL-15] cells frequently contain a minor fraction ($< 10\%$) of cells that are L-selectin⁻ and/or CCR7⁻ and phenotypically more similar to CD8[IL-2] cells (18). Thus, it was important to determine whether the homed CD8[IL-15] cells in the peritoneal cavity were representative of the bulk of the input population. Flow cytometric analysis of CD8[IL-15] cells recovered from PEL showed that nearly all cells were L-selectin⁺ and responded to CCL21 in chemotaxis assays (data not shown). Thus, CD8[IL-15] cells possess not only the capacity to home to secondary lymphoid organs, but also to sites of inflammation. In contrast, CD8[IL-2] cells home even more avidly to inflamed tissues, but they are excluded from entry into secondary lymphoid organs except the spleen.

CD8[IL-15] Cells Proliferate Rapidly in Response to Recall Antigen at Sites of Inflammation. We next assessed whether CD8[IL-15] cells would respond to antigen encounter at sites of inflammation. To this end, 2.5×10^7 CFSE-labeled CD8[IL-15] cells from P14 mice were adoptively transferred into C57BL/6 mice. 24 h later, two groups of three animals each received an intraperitoneal injection of emulsified IFA without or with gp33 peptide (50 μg). After 72 h, cells were harvested from the peritoneal cavity, PLNs, and MLNs. As the degree of inflammation and, consequently, the number of homed cells in PEL was quite variable, we determined the percentage of CFSE⁺ cells in the total CD8⁺ T cell population in each animal. The frequency of CD8⁺CFSE⁺ cells in PLNs tended to be somewhat lower in mice challenged with antigen, compared with mice that received no peptide (PLNs: $9.0 \pm 2.7\%$ vs. $4.6 \pm 1.2\%$; $P = 0.22$; MLNs: $10.4 \pm 4.3\%$ vs. $7.4 \pm 1.6\%$; $P = 0.23$; Fig. 8 A). In contrast, the presence of cognate antigen markedly increased the number of CD8[IL-15] cells at the site of challenge; there were seven times more CFSE⁺ cells in the PEL of gp33 challenged as compared with control animals ($18.2 \pm 3.6\%$ vs. $2.6 \pm 1.0\%$; $P = 0.01$). Importantly, there was a considerable loss of CFSE staining among homed CD8[IL-15] cells recovered from the PEL, but not from PLNs of the same animal (Fig. 8 B). This indicates that many CD8[IL-15] cells that were exposed to antigen in the peritoneal cavity proliferated at this site.
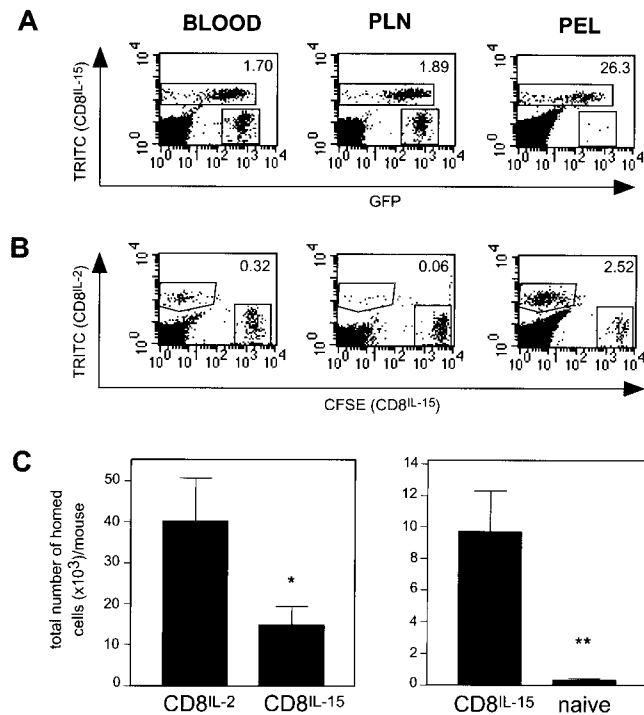
Figure 7. CD8[IL-2] and CD8[IL-15], but not naive T cells are recruited to sites of inflammation. Peritonitis was induced by injection of IFA into the peritoneal cavity of C57BL/6 mice. 72 h later, one group ($n = 6$ animals) received 2.5×10^7 TRITC-labeled CD8[IL-15] mixed with 4×10^7 freshly isolated T-GFP splenocytes (A). A second group ($n = 8$ mice) received an equivalent number (2.5×10^7 cells of each) of TRITC-labeled CD8[IL-2] cells and CFSE-labeled CD8[IL-15] cells (B). Representative two-color dot plots show the frequency of fluorescent CD8[IL-15] versus T-GFP cells (A) and of CD8[IL-2] versus CD8[IL-15] cells (B) in blood, PLNs, and peritoneal exudate leukocytes (PEL). Numbers in the upper right corner of each histogram represent the ratio of CD8[IL-15]:naive T-GFP cells (A) or of CD8[IL-2]:CD8[IL-15] cells (B). (C) Bars represent the mean $\pm$ SEM of the absolute numbers of homed cells recovered from inflamed peritoneal cavities. Statistical differences were assessed using the unpaired Student's *t* test. *$P < 0.05$; **$P < 0.01$.

Discussion

We have recently observed that exposure of activated murine CD8⁺ T cells to IL-2 or IL-15 modulates their differentiation into distinct populations that are essentially indistinguishable from effector CTL and a subset of memory
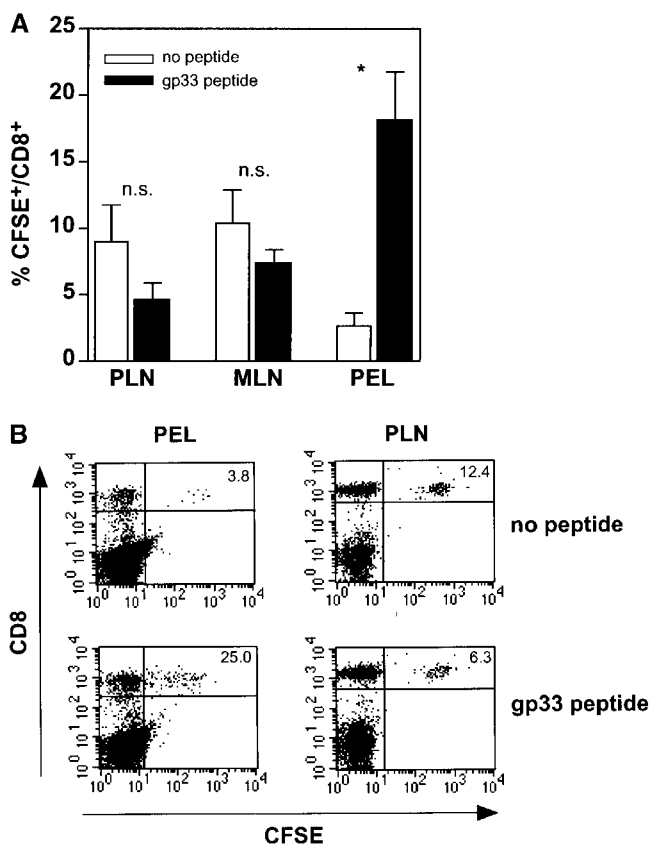
Figure 8. CD8^IL-15 cells proliferate in the peritoneal cavity in the presence of peptide antigen. 2.5×10^7 CFSE labeled CD8^IL-15 cells from P14 mice were injected into C57BL/6 mice. 24 h later, peritonitis was induced by intraperitoneal injection of IFA without or with gp33 peptide (50 μg). After 72 h, PEL and LN cells were harvested, stained, and analyzed by FACS®. (A) Shows the percentage of CFSE^+ cells in the total CD8^+ population in each organ. Bars represent mean ± SEM from three animals. Values for each organ were compared using the Student's *t* test (n.s., not significant; *$P = 0.01$). (B) Representative FACS® dotplots of PLNs and PEL from animals receiving intraperitoneal injection of IFA without (top two plots) or with gp33 peptide (bottom two plots). The number in the right corner represents the percentage of CFSE^+ cells in the CD8^+ population.

cells, respectively (18). Here, we have examined the effects of these two cytokines on T cell trafficking. Naive T cells homed efficiently to lymphoid organs and were attracted by CCL21, but they did not migrate to inflamed peritoneum or respond to inflammatory chemokines. In contrast, CD8^IL-2 cells accumulated at a high frequency in the inflamed peritoneal cavity and entered the spleen, but homed poorly to LNs and PPs. CD8^IL-15 cells migrated moderately to inflamed peritoneum, where they were capable of proliferation in response to antigen. Furthermore, they homed to LNs and PPs similar to naive cells and migrated more avidly to the spleen than naive or CD8^IL-2 cells. These findings are consistent with established concepts of naive T cell homing (1, 2) and a previous report on CD8^+ effector cell migration (42). To our knowledge, this is the first study on the migratory behavior of long-lived memory cells that share key features with so-called central memory cells (18, 27).

A major obstacle to definitive investigations of memory cell migration has been the lack of distinct markers for effector versus memory cells. Moreover, long-lived memory cells are fairly rare and heterogeneous in vivo, which makes it hard to isolate and study them. Aside from functional differences between CD4^+ and CD8^+ cells, there are probably numerous effector memory subsets with distinct migratory preferences. Thus, to examine the homing behavior of more homogenous populations, several recent studies used adoptive transfer of in vitro differentiated cells, particularly short-term stimulated CD4^+ cells (43) and polarized Th1 and Th2 cells, which follow discrete, subset-specific traffic signals (44–48). Similar experiments suggest that CD8^+ effector cells can also acquire diverse migratory properties (42, 49). While significant knowledge of effector cell migration has been gathered in these studies, the migratory behavior of long-lived memory CD8^+ T cells has not been investigated in a similar fashion, because it has been difficult to generate such cells in vitro. Thus, our current concept of memory cell migration is largely based on histological studies that provide a snapshot of cellular localization within the body (23), but provide limited information about the migratory mechanisms and kinetics or cellular turnover within tissues.

Antigen-experienced CD8^+ T cells in mice that underwent viral infections were found to be either L-selectin^+ or L-selectin^- suggesting that two distinct memory cell populations may exist (50). More recently, it was shown that CD45RA^- T cells in peripheral blood of healthy human donors as well as in individuals with persistent EBV-infection also consist of two major populations that are separable by their differential expression of CCR7 and L-selectin (27, 51). Based on the known role for these two molecules in lymphocyte homing to LNs, it was proposed that the CCR7^+ L-selectin^+ "central memory cells" home to lymphoid organs, whereas the CCR7^- L-selectin^- "effector memory cells" may possess diverse migratory specificities for nonlymphoid tissues. CD8^IL-15 cells from T-GFPxP14 mice show a strikingly similar phenotype and function as human "central memory" cells (18). The migratory behavior of CD8^IL-15 cells presented in this paper provides strong support to another key feature of "central memory cells" that had been postulated (27), but has not been shown experimentally; within hours after adoptive transfer CD8^IL-15 cells homed avidly to all lymphoid tissues in recipient mice. Most CD8^IL-15 cells remained in lymphoid organs for at least several weeks, but a small number of cells was also found in the circulation (data not shown). This pattern is consistent with the notion that central memory cells may stand guard in LNs to orchestrate antigen specific recall responses, but a fraction may constantly recirculate between blood and lymphoid organs analogous to the well-described immune surveillance by naive T cells (1).

24 h homing assays revealed that, after accounting for differences in the number of injected cells, naive T cells were ~2.5-fold more frequent in blood than CD8^IL-2 or CD8^IL-15 cells. The same ratio was seen at 3 h after injection and even fewer cytokine-treated cells circulated at ear-

lier time points; at 5 min after injection, nearly 100 times more T-GFP cells than cytokine-treated cells were found in the blood (data not shown). This suggests that the latter were delayed and/or retained during their passage through pulmonary microvessels. In addition, a substantial number of CD8^{IL-2} cells and, to a lesser extent, CD8^{IL-15} cells were found in the liver. As these cells must have passed through pulmonary capillaries, they were probably sufficiently small and/or deformable to pass through hepatic sinuses and capillaries as well. Thus, their retention in the liver probably involved specific adhesion events. The molecular mechanisms for such a putative liver-specific homing pathway and the immunologic consequences of CD8^{IL-2} and CD8^{IL-15} cell migration to the liver will require further studies.

The sequestration of CD8^{IL-2} and CD8^{IL-15} cells, but not naive T cells in lung and liver makes the interpretation of homing indices in lymphoid tissues more difficult. For example the homing index of CD8^{IL-15} cells in the spleen was ~1.5, indicating that 50% more CD8^{IL-15} cells than naive cells reached that organ after intravenous injection. Previous studies have found a similar magnitude of naive and memory cell homing to the spleen (46, 52). However, due to differential sequestration, ~2.5-fold more naive than CD8^{IL-15} cells are blood-borne leading to a disproportionate delivery of the two subsets to peripheral organs. If one corrects for this difference in circulating cell numbers, CD8^{IL-15} cells actually accumulated ~3.2 times more efficiently in the spleen than naive T cells, whereas CD8^{IL-2} cells homed to the spleen with comparable efficiency as naive T cells. Interestingly, splenocytes of unchallenged T-GFP mice contain a GFP$^-$ CD8$^+$ T cell population that consists entirely of CD44^{hi} T cells. Similar to our finding with blood-borne memory cells (Table II), the splenic GFP$^-$ population represents ~35% of all CD44^{hi}CD8$^+$ splenocytes and is mostly L-selectin$^{-/low}$, while ~75% of the GFP$^+$CD44^{hi}CD8$^+$ memory cells are L-selectin$^+$. The frequency of both endogenous CD8$^+$ memory populations in the spleen and blood increases with the animals' age, but the ratio of GFP$^+$ to GFP$^-$ memory cells remains fairly constant (i.e. ~2:1). This splenic ratio is remarkably similar to the relative spleen homing capacity of CD8^{IL-15} cells and CD8^{IL-2} cells, which are also GFP$^+$L-selectin$^+$ and GFP$^-$L-selectin$^-$, respectively.

Immunofluorescence staining of spleen sections showed that nearly all CD8^{IL-15} cells localized within the PALS, whereas ~40% of CD8^{IL-2} cells were found outside the T cell areas. Similarly, a recent study found that in vitro activated LCMV-specific CTLs homed to both the red pulp and PALS (53). It is believed that T cells enter the spleen in the red pulp and must actively migrate to reach the PALS. Therefore, it is unlikely that CD8^{IL-15} and CD8^{IL-2} cells were only passively trapped within splenic compartments. Interestingly, the distribution of homed CD8^{IL-15} cells in the spleen coincides with that of lymphoid (CD8α^+) DCs, which are concentrated in the PALS, whereas myeloid DCs are preferentially found within and close to the red pulp (54). As these two DC subsets are thought to orchestrate immunologically distinct T cell responses (55, 56), it is

possible that central memory and effector T cells receive different signals and perform distinct functions in the spleen. For example, colocalization of myeloid DCs with CTLs in the red pulp may allow the elimination of DCs that contain live pathogens, whereas lymphoid DC that are sheltered in the PALS may cross-prime naive and central memory CD8α^+ cells to antigens transferred from other cells (56).

While the traffic signals for CD8$^+$ subsets in the spleen remain to be identified, the dramatic (~20-fold) difference in homing of CD8^{IL-15} versus CD8^{IL-2} cells to PLNs and MLNs can be explained at the molecular level. When taking in account the different frequencies of adoptively transferred cells in systemic blood (see above), CD8^{IL-15} cells migrated to LNs with equal efficiency as naive T cells. The adhesion cascades that mediate naive T cell homing to LNs and PPs are well understood (for a review, see reference 2). L-selectin is crucial for tethering and rolling in HEVs, the first essential steps during homing to LNs. L-selectin$^{-/-}$ mice have hypocellular LNs and their lymphocytes do not home to LNs of wild-type mice (7). Accordingly, L-selectin$^+$ wild-type CD8^{IL-15} cells rolled in PLN HEVs, whereas CD8^{IL-15} cells from T-GFPxL$^{-/-}$ mice did not home to LNs. Thus, L-selectin is necessary for both naive and CD8^{IL-15} cell homing to LNs. As most CD8^{IL-2} cells are L-selectin$^{low/-}$ it is not surprising that they failed to accumulate in LNs. The small fraction of CD8^{IL-2} cells that rolled in HEVs probably belonged to a subset of L-selectin$^+$ CD8^{IL-2} cells that were present in most cultures (Table I; reference 18). However, we cannot exclude alternative mechanisms such as bridging by activated platelets, whose surface expressed P-selectin binds to PNAd on HEVs and to appropriately glycosylated P-selectin glycoprotein ligand-1 (PSGL-1) on circulating lymphocytes (57). This possibility is supported by the finding that P-selectin ligands are upregulated on CD8^{IL-2} cells (Table I).

Irrespective of the mechanism(s) by which a T cell rolls in HEVs, it can only home to PLNs after engaging LFA-1 to arrest firmly (8, 58). Several studies have shown that CCL21 (and possibly CCL19) signaling through CCR7 provides a crucial integrin activating stimulus to naive T cells (9, 10, 14). As CCR7 is expressed on CD8^{IL-15} cells, but not on CD8^{IL-2} cells (18), and only the former migrated to CCL21 in chemotaxis assays, it seemed plausible that their differential homing to secondary lymphoid tissues was due, in part, to their distinct responsiveness to CCR7 agonists. Indeed, the number of homed CD8^{IL-15} cells in PLNs of plt/plt mice was ~80% lower than in wild-type recipients.

Despite their differential ability to respond to CCL21, we found that the two subsets of antigen–experienced cells responded to inflammatory chemokines in chemotaxis assays. Earlier studies have found that in vitro polarized Tc1 cells express high levels of CCR2 and CCR5, whereas Tc2 cells expressed more CCR1 (49). CCR2 and CCR5 are also highly expressed on CD8$^+$ effector cells that accumulate at sites of LCMV infection (59). In good agreement with these studies, we found that CD8^{IL-2} cells responded strongly to CCL2, a CCR2 agonist, and CCL5, a CCR5

agonist, whereas naive T cells were insensitive to these chemokines. Interestingly, CD8^{IL-15} cells had an intermediate phenotype; they responded not only to CCL21, but also to CCL5, and CCL2 (although somewhat more weakly than CD8^{IL-2} cells). Of note, coexpression of CCR7 and inflammatory chemokine receptors has also been observed on central memory cells in humans (27), suggesting yet another shared feature of central memory cells and CD8^{IL-15} cells.

The induction of inflammatory chemokine receptors on CD8^{IL-2} cells as well as their de novo expression of P-selectin ligands (Table I) suggested that CD8^{IL-2} cells had acquired the ability to migrate to sites of inflammation. To test this hypothesis, we employed a model of IFA induced peritonitis, which has been used previously to study the migration of naive T cells and polarized Th1, Th2, and Tc1 cells (42). After correcting for differences in circulating cell counts, CD8^{IL-2} cells migrated nearly 12 times more frequently to the peritoneal cavity than CD8^{IL-15} cells, and ~15 times more CD8^{IL-15} cells than naive T cells were recovered from this site. Although we cannot exclude that some cytokine-treated cells divided in the peritoneal cavity, it seems unlikely that differential proliferation of homed subsets had a major impact on these results since CD8^{IL-15} and CD8^{IL-2} cells proliferate at similar rates in vitro (18). Moreover, another study in this model has found little proliferation of homed effector T cells in the absence of specific antigen (42).

The observed hierarchy of migratory preferences, with CD8^{IL-2} cells having the highest, CD8^{IL-15} cells a moderate, and naive T cells virtually no ability to enter sites of inflammation, is consistent with the armamentarium of traffic molecules expressed by each subset. In contrast to naive T cells, both CD8^{IL-2} and CD8^{IL-15} cells expressed not only inflammatory chemokine receptors, but also increased levels of CD44, α4 integrins, and LFA-1 (Table I; reference 18, and data not shown), which are necessary for efficient lymphocyte migration to sites of inflammation (5, 60). However, only CD8^{IL-2} cells, but not CD8^{IL-15} cells displayed detectable P-selectin ligands, whose expression correlates with the ability of CD8$^+$ T cells and Th1 cells to migrate to inflamed tissues (42). Thus, we speculate that the difference in homing to inflamed peritoneum between CD8^{IL-2} and CD8^{IL-15} cells was due to differential expression of α-1,3-fucosyltransferase (FucT)-VII and possibly FucT-IV and/or core 2 β-1,6-N-acetylglycosaminyl-transferase, which are required for leukocyte expressed selectin ligand activity in vivo (61–63).

The capacity of CD8^{IL-15} cells to home directly to sites of inflammation suggested that central memory cells may not exert their immunological function exclusively by recirculating through secondary lymphoid organs. It was therefore important to demonstrate that these cells can respond to cognate antigen at nonlymphoid effector sites. Indeed, in the presence of antigenic peptide, considerably more cells were recovered from the inflamed peritoneal cavity than in its absence. There are two nonexclusive explanations for the higher cell yield: either the cells proliferated locally in

response to antigen or more cells were recruited from the blood stream. We favor the first explanation, since many PEL cells had lower CFSE intensities than cells recovered from LNs of the same animal or from PEL of control animals. Moreover, these results are in line with data presented by Xie et al., who also demonstrated local proliferation of Th1 cells in the peritoneal cavity in the presence of antigen (42).

An important question is whether and to what extent antigen-experienced T cells that arise in vivo resemble in vitro generated CD8^{IL-15} or CD8^{IL-2} cells. As mentioned above, endogenous CD8$^+$ memory cells in blood and spleen of T-GFP mice consist of two populations that are either GFP$^+$ (~70%) or GFP$^-$ (~30%). Expression of GFP on these cells appears to be correlated with L-selectin and CCR7 expression (Table II, and data not shown). Nearly all cells in the GFP$^+$ subset coexpress L-selectin and CCR7 and thus resemble central memory cells found in humans. In contrast, L-selectin and CCR7 are mostly absent on GFP$^-$ memory cells. In addition, we have shown previously that virtually all CD8$^+$ effector CTLs in the PEL of T-GFP mice with experimental peritonitis are GFP$^-$ (15). Thus, the organ distribution and L-selectin/CCR7 expression of endogenous GFP$^+$ and GFP$^-$ subsets are mirrored in the differential trafficking of CD8^{IL-15} memory and CD8^{IL-2} effector cells, respectively. However, further characterization of endogenous T cell subsets in T-GFP mice will be necessary to assess the parallels and potential differences of in vivo and in vitro generated antigen-experienced T cells, especially in the GFP$^-$ compartment.

Taken together, our studies on CD8^{IL-15} cells support and expand the concept that different antigen-experienced T cell populations exist that possess distinct migratory properties. While the propensity of effector cells for inflamed tissues has been noted previously, this is the first report on the migratory routes of CD8$^+$ central memory-like cells. This memory population follows the traffic pattern of naive T cells by recirculating through secondary lymphoid organs in search for cognate antigen. As this memory subset differs from effector cells in that it does not exert immediate cytotoxicity, its presence in lymphoid tissues may not pose an imminent threat to resident APCs. However, as would be expected from a bona fide memory cell, CD8^{IL-15} cells that are exposed to TCR stimulation differentiate rapidly into effector cells (18). Furthermore, central memory cells are capable of entering peripheral sites of inflammation. It seems likely that local exposure to antigen in inflamed tissues would stimulate central memory cells to give rise to large numbers of effector cells. This would reduce the need for antigen transport and presentation in draining LNs and, thus, accelerate the elimination of antigen at its source.

References

1. Butcher, E.C., and L.J. Picker. 1996. Lymphocyte homing and homeostasis. *Science*. 272:60–66.
2. von Andrian, U.H., and C.R. Mackay. 2000. T-cell function and migration. Two sides of the same coin. *N. Engl. J. Med.* 343:1020–1034.
3. Kagi, D., B. Ledermann, K. Burki, R.M. Zinkernagel, and H. Hengartner. 1996. Molecular mechanisms of lymphocyte-mediated cytotoxicity and their role in immunological protection and pathogenesis in vivo. *Annu. Rev. Immunol.* 14:207–232.
4. Clark, W.R., C.M. Walsh, A.A. Glass, F. Hayashi, M. Matloubian, and R. Ahmed. 1995. Molecular pathways of CTL-mediated cytotoxicity. *Immunol. Rev.* 146:33–44.
5. Springer, T.A. 1994. Traffic signals for lymphocyte recirculation and leukocyte emigration: The multi-step paradigm. *Cell*. 76:301–314.
6. Gallatin, W.M., I.L. Weissman, and E.C. Butcher. 1983. A cell-surface molecule involved in organ-specific homing of lymphocytes. *Nature*. 304:30–34.
7. Arbonés, M.L., D.C. Ord, K. Ley, H. Ratech, C. Maynard-Curry, G. Otten, D.J. Capon, and T.F. Tedder. 1994. Lymphocyte homing and leukocyte rolling and migration are impaired in L-selectin-deficient mice. *Immunity*. 1:247–260.
8. Warnock, R.A., S. Askari, E.C. Butcher, and U.H. von Andrian. 1998. Molecular mechanisms of lymphocyte homing to peripheral lymph nodes. *J. Exp. Med.* 187:205–216.
9. Förster, R., A. Schubel, D. Breitfeld, E. Kremmer, I. Renner-Muller, E. Wolf, and M. Lipp. 1999. CCR7 coordinates the primary immune response by establishing functional microenvironments in secondary lymphoid organs. *Cell*. 99:23–33.
10. Gunn, M.D., S. Kyuwa, C. Tam, T. Kakiuchi, A. Matsuzawa, L.T. Williams, and H. Nakano. 1999. Mice lacking expression of secondary lymphoid organ chemokine have defects in lymphocyte homing and dendritic cell localization. *J. Exp. Med.* 189:451–460.
11. Andrew, D.P., J.P. Spellberg, H. Takimoto, R. Schmits, T.W. Mak, and M.M. Zukowski. 1998. Transendothelial migration and trafficking of leukocytes in LFA-1-deficient mice. *Eur. J. Immunol.* 28:1959–1969.
12. Berlin-Rufenach, C., F. Otto, M. Mathies, J. Westermann, M.J. Owen, A. Hamann, and N. Hogg. 1999. Lymphocyte migration in lymphocyte function-associated antigen (LFA)-1–deficient mice. *J. Exp. Med.* 189:1467–1478.
13. Warnock, R.A., J.J. Campbell, M.E. Dorf, A. Matsuzawa, L.M. McEvoy, and E.C. Butcher. 2000. The role of chemokines in the microenvironmental control of T versus B cell arrest in Peyer's patch high endothelial venules. *J. Exp. Med.* 191:77–88.
14. Stein, J.V., A. Rot, Y. Luo, M. Narasimhaswamy, H. Nakano, M.D. Gunn, A. Matsuzawa, E.J. Quackenbush, M.E. Dorf, and U.H. von Andrian. 2000. The CC chemokine thymus-derived chemotactic agent 4 (TCA-4, secondary lymphoid tissue chemokine, 6Ckine, exodus-2) triggers lymphocyte function-associated antigen 1–mediated arrest of rolling T lymphocytes in peripheral lymph node high endothelial venules. *J. Exp. Med.* 191:61–76.
15. Manjunath, N., P. Shankar, B. Stockton, P.D. Dubey, J. Lieberman, and U.H. von Andrian. 1999. A transgenic mouse model to analyze CD8+ effector T cell differentiation in vivo. *Proc. Natl. Acad. Sci. USA*. 96:13932–13937.
16. Harrington, L.E., M. Galvan, L.G. Baum, J.D. Altman, and R. Ahmed. 2000. Differentiating between memory and effector CD8 T cells by altered expression of cell surface O-glycans. *J. Exp. Med.* 191:1241–1246.
17. Pircher, H., K. Burki, R. Lang, H. Hengartner, and R.M. Zinkernagel. 1989. Tolerance induction in double specific T-cell receptor transgenic mice varies with antigen. *Nature*. 342:559–561.
18. Manjunath, N., P. Shankar, J. Wan, W. Weninger, M.A. Crowley, K. Hieshima, T.A. Springer, X. Fan, H. Shen, J. Lieberman, and U.H. von Andrian. 2001. Effector differentiation is not prerequisite for generation of memory cytotoxic T lymphocytes. *J. Clin. Invest.* 108:871–878.
19. Sprent, J. 1994. T and B memory cells. *Cell*. 76:315–322.
20. Ahmed, R., and D. Gray. 1996. Immunological memory and protective immunity: understanding their relation. *Science*. 272:54–60.
21. Dutton, R.W., L.M. Bradley, and S.L. Swain. 1998. T cell memory. *Annu. Rev. Immunol.* 16:201–223.
22. Reinhardt, R.L., A. Khoruts, R. Merica, T. Zell, and M.K. Jenkins. 2001. Visualizing the generation of memory CD4 T cells in the whole body. *Nature*. 410:101–105.
23. Masopust, D., V. Vezys, A.L. Marzo, and L. Lefrancois. 2001. Preferential localization of effector memory cells in nonlymphoid tissue. *Science*. 291:2413–2417.
24. Mackay, C.R., W.L. Marston, and L. Dudler. 1990. Naive and memory T cells show distinct pathways of lymphocyte recirculation. *J. Exp. Med.* 171:801–817.
25. Mackay, C.R. 1991. T-cell memory: the connection between function, phenotype and migration pathways. *Immunol. Today*. 12:189–192.
26. Westermann, J., and R. Pabst. 1996. How organ-specific is the migration of 'naive' and 'memory' T cells? *Immunol. Today*. 17:278–282.
27. Sallusto, F., D. Lenig, R. Forster, M. Lipp, and A. Lanzavecchia. 1999. Two subsets of memory T lymphocytes with distinct homing potentials and effector functions. *Nature*. 401:708–712.
28. Ku, C.C., M. Murakami, A. Sakamoto, J. Kappler, and P. Marrack. 2000. Control of homeostasis of CD8+ memory T cells by opposing cytokines. *Science*. 288:675–678.
29. Catalina, M.D., M.C. Carroll, H. Arizpe, A. Takashima, P. Estess, and M.H. Siegelman. 1996. The route of antigen entry determines the requirement for L-selectin during immune responses. *J. Exp. Med.* 184:2341–2351.
30. von Andrian, U.H. 1996. Intravital microscopy of the peripheral lymph node microcirculation in mice. *Microcirculation*. 3:287–300.
31. von Andrian, U.H., and C. M'Rini. 1998. In situ analysis of lymphocyte migration to lymph nodes. *Cell. Adhes. Commun.* 6:85–96.
32. Butcher, E.C., and W.L. Ford. 1986. Following cellular traffic: methods of labelling lymphocytes and other cells to trace

their migration *in vivo*. 4th ed. *In* Handbook of Experimental Immunology, Volume 2: Cellular Immunology. D.M. Weir, L.A. Herzenberg, and C. Blackwell, editors. Blackwell Scientific Publications, London. 57.51–57.23.

33. Cyster, J.G., and C.C. Goodnow. 1995. Pertussis toxin inhibits migration of B and T lymphocytes into splenic white pulp cords. *J. Exp. Med.* 182:581–586.

34. Randolph, D.A., G. Huang, C.J. Carruthers, L.E. Bromley, and D.D. Chaplin. 1999. The role of CCR7 in TH1 and TH2 cell localization and delivery of B cell help in vivo. *Science*. 286:2159–2162.

35. Gunn, M.D., K. Tangemann, C. Tam, J.G. Cyster, S.D. Rosen, and L.T. Williams. 1998. A chemokine expressed in lymphoid high endothelial venules promotes the adhesion and chemotaxis of naive T lymphocytes. *Proc. Natl. Acad. Sci. USA*. 95:258–263.

36. Zlotnik, A., and O. Yoshie. 2000. Chemokines: a new classification system and their role in immunity. *Immunity*. 12: 121–127.

37. Nakano, H., S. Mori, H. Yonekawa, H. Nariuchi, A. Matsuzawa, and T. Kakiuchi. 1998. A novel mutant gene involved in T-lymphocyte-specific homing into peripheral lymphoid organs on mouse chromosome 4. *Blood*. 91:2886–2895.

38. Vassileva, G., H. Soto, A. Zlotnik, H. Nakano, T. Kakiuchi, J.A. Hedrick, and S.A. Lira. 1999. The reduced expression of 6Ckine in the plt mouse results from the deletion of one of two 6Ckine genes. *J. Exp. Med.* 190:1183–1188.

39. Luther, S.A., H.L. Tang, P.L. Hyman, A.G. Farr, and J.G. Cyster. 2000. Coexpression of the chemokines ELC and SLC by T zone stromal cells and deletion of the ELC gene in the plt/plt mouse. *Proc. Natl. Acad. Sci. USA*. 97:12694–12699.

40. Nakano, H., T. Tamura, T. Yoshimoto, H. Yagita, M. Miyasaka, E.C. Butcher, H. Nariuchi, T. Kakiuchi, and A. Matsuzawa. 1997. Genetic defect in T lymphocyte-specific homing into peripheral lymph nodes. *Eur. J. Immunol.* 27: 215–221.

41. Sallusto, F., C.R. Mackay, and A. Lanzavecchia. 2000. The role of chemokine receptors in primary, effector, and memory immune responses. *Annu. Rev. Immunol.* 18:593–620.

42. Xie, H., Y.C. Lim, F.W. Luscinskas, and A.H. Lichtman. 1999. Acquisition of selectin binding and peripheral homing properties by CD4+ and CD8+ T cells. *J. Exp. Med.* 189: 1765–1776.

43. Iezzi, G., D. Scheidegger, and A. Lanzavecchia. 2001. Migration and function of antigen-primed nonpolarized T lymphocytes in vivo. *J. Exp. Med.* 193:987–993.

44. Austrup, F., D. Vestweber, E. Borges, M. Lohning, R. Brauer, U. Herz, H. Renz, R. Hallman, A. Scheffold, A. Radbruch, and A. Hamann. 1997. P- and E-selectin mediate recruitment of T-helper-1 but not T-helper-2 cells into inflammed tissues. *Nature*. 385:81–83.

45. Borges, E., W. Tietz, M. Steegmaier, T. Moll, R. Hallmann, A. Hamann, and D. Vestweber. 1997. P-selectin glycoprotein ligand-1 (PSGL-1) on T helper 1 but not on T helper 2 cells binds to P-selectin and supports migration into inflamed skin. *J. Exp. Med.* 185:573–578.

46. Tietz, W., and A. Hamann. 1997. The migratory behavior of murine CD4 cells of memory phenotype. *Eur. J. Immunol.* 27:2225–2232.

47. Syrbe, U., J. Siveke, and A. Hamann. 1999. Th1/Th2 subsets: distinct differences in homing and chemokine receptor expression? *Springer Semin. Immunopathol.* 21:263–285.

48. Hamann, A., K. Klugewitz, F. Austrup, and D. Jablonski-Westrich. 2000. Activation induces rapid and profound alterations in the trafficking of T cells. *Eur. J. Immunol.* 30:3207–3218.

49. Cerwenka, A., T.M. Morgan, A.G. Harmsen, and R.W. Dutton. 1999. Migration kinetics and final destination of type 1 and type 2 CD8 effector cells predict protection against pulmonary virus infection. *J. Exp. Med.* 189:423–434.

50. Oehen, S., and K. Brduscha-Riem. 1998. Differentiation of naive CTL to effector and memory CTL: correlation of effector function with phenotype and cell division. *J. Immunol.* 161:5338–5346.

51. Tussey, L., S. Speller, A. Gallimore, and R. Vessey. 2000. Functionally distinct CD8+ memory T cell subsets in persistent EBV infection are differentiated by migratory receptor expression. *Eur. J. Immunol.* 30:1823–1829.

52. Williams, M.B., and E.C. Butcher. 1997. Homing of naive and memory T lymphocyte subsets to Peyer's patches, lymphnodes, and spleen. *J. Immunol.* 159:1746–1752.

53. Potsch, C., D. Vohringer, and H. Pircher. 1999. Distinct migration patterns of naive and effector CD8 T cells in the spleen: correlation with CCR7 receptor expression and chemokine reactivity. *Eur. J. Immunol.* 29:3562–3570.

54. Steinman, R.M., M. Pack, and K. Inaba. 1997. Dendritic cells in the T-cell areas of lymphoid organs. *Immunol. Rev.* 156:25–37.

55. Banchereau, J., and R.M. Steinman. 1998. Dendritic cells and the control of immunity. *Nature*. 392:245–252.

56. den Haan, J.M.M., S.M. Lehar, and M.J. Bevan. 2000. CD8+ but not CD8− dendritic cells cross-prime cytotoxic T cells in vivo. *J. Exp. Med.* 192:1685–1695.

57. Diacovo, T.G., M.D. Catalina, M.H. Siegelman, and U.H. von Andrian. 1998. Circulating activated platelets reconstitute lymphocyte homing and immunity in L-selectin-deficient mice. *J. Exp. Med.* 187:197–204.

58. Hamann, A., D.J. Westrich, A. Duijevstijn, E.C. Butcher, H. Baisch, R. Harder, and H.G. Thiele. 1988. Evidence for an accessory role of LFA-1 in lymphocyte-high endothelium interaction during homing. *J. Immunol.* 140:693–699.

59. Nansen, A., O. Marker, C. Bartholdy, and A.R. Thomsen. 2000. CCR2+ and CCR5+ CD8+ T cells increase during viral infection and migrate to sites of infection. *Eur. J. Immunol.* 30:1797–1806.

60. Degrendele, H.C., P. Estess, and M.H. Siegelman. 1997. Requirement for CD44 in activated T cell extravasation into an inflammatory site. *Science*. 278:672–675.

61. Maly, P., A.D. Thall, B. Petryniak, C.E. Rogers, P.L. Smith, R.M. Marks, R.J. Kelly, K.M. Gersten, G. Cheng, T.L. Saunders, et al. 1996. The $\alpha(1,3)$ fucosyltransferase Fuc-TVII controls leukocyte trafficking through an essential role in L-, E-, and P-selectin ligand biosynthesis. *Cell*. 86:643–653.

62. Ellies, L.G., S. Tsuboi, B. Petryniak, J.B. Lowe, M. Fukuda, and J.D. Marth. 1998. Core 2 oligosaccharide biosynthesis distinguishes between selectin ligands essential for leukocyte homing and inflammation. *Immunity*. 9:881–890.

63. Weninger, W., L.H. Ulfman, G. Cheng, N. Souchkova, E.J. Quackenbush, J.B. Lowe, and U.H. von Andrian. 2000. Specialized contributions by alpha(1,3)-fucosyltransferase-IV and FucT-VII during leukocyte rolling in dermal microvessels. *Immunity*. 12:665–676.